Desalination and Water Treatment
www.deswater.com

doi: 10.5004/dwt.2021.26649

214 (2021) 86–94
February

Polyethersulfone-co-polyesters blend ultrafiltration membranes for biomedical and biotechnological applications. Preliminary study

Andrzej Chwojnowski[a,*], Cezary Wojciechowski[a], Monika Wasyłeczko[a], Ewa Łukowska[a], Tomasz Kobiela[b], Piotr Dobrzyński[c], Małgorzata Pastusiak[c], Anna Smola-Dmochowska[c]

[a]*Institute of Biocybernetic and Biomedical Engineering, PAS 02-109 Warszawa, Trojdena str. 4, Poland, emails: achwojnowski@ibib.waw.pl (A. Chwojnowski), wojciechowski@ibib.waw.pl (C. Wojciechowski), mwasyleczko@ibib.waw.pl (M. Wasyłeczko), elukowska@ibib.waw.pl (E. Łukowska)*
[b]*Faculty of Chemistry Warsaw University of Technology, 00-664 Warszawa, Noakowskiego str. 3, Poland, email: kobiela@ch.pw.edu.pl*
[c]*Centre of Polymer and Carbon Materials, PAS 41-819 Zabrze, M. Curie-Skłodowskiej str. 34, Poland, emails: pdobrzynski@cmpw-pan.edu.pl (P. Dobrzynski), mpastusiak@cmpw-pan.edu.pl (M. Pastusiak), asmola@cmpw-pan.edu.pl (A. Smola-Dmochowska)*

Received 28 February 2020; Accepted 25 May 2020

ABSTRACT

Polyethersulfone (PES) L-lactide/glycolide/ε-caprolactone (LGC) terpolymer blend ultrafiltration membranes were prepared by non-solvent-induced phase separation method using macromolecular additives – polyvinylpyrrolidone and Pluronic® 127. The membrane forming mixtures were prepared by mixing two solutions: PES in *N*-methyl-2-pyrrolidone and LGC in tetrahydrofuran. The membranes before and after hydrolysis were characterized by: Fourier transform infrared, contact angle, scanning electron microscopy, atomic force microscopy, elemental analysis, hydraulic permeability, and cut-off point. The hydrolysis of LGC terpolymer component in the membranes was tested by the gravimetric method. The changes of properties of membranes due to the hydrolysis were investigated. Hydrolysis was carried out for 46 weeks. The cut-off point of membranes did not change significantly after hydrolysis. A significant increase in hydraulic permeability ranging from 32% to 48% depending on the membrane was detected.

Keywords: Polyethersulfone; Terpolymer; Ultrafiltration membrane; Blend membrane

1. Introduction

Biocompatible membranes have numerous potential biological and medical applications that involve isolating, biosorting, releasing, or immobilization biological molecules including cells, and even using for cell culture [1–5]. Exactly in tissue engineering (TE), various forms of the semipermeable membrane are used to produce functional substitutes for damaged tissues or entire organs [6–9]. One of the method is transplantation cells which were previously encapsulated. Encapsulation technology includes the surrounding of living cells within semipermeable membranes to protect them from immune destruction. Furthermore, it allows the bidirectional diffusion of nutrients, oxygen, and the release of waste and therapeutic molecules outside membranes. Technology is a promising strategy for treating a wide range of human diseases, like

* Corresponding author.

acute liver failure, diabetes, spinal cord injury, blood disorders, and even several types of cancer [10–12]. Cell encapsulation allows the transplantation of non-human cells which could be considered as an alternative to the limited supply of donor tissue [11]. In addition, genetically modified cells can be immobilized to express any desired protein *in vivo* without the modification of the host's genome [11,13,14]. Microencapsulation system is one of the cell encapsulation technique where can be used many methods like dropping, coacervation (often called co-extrusion), complex coacervation, spraying, interfacial polymerization, layer-by-layer method, moulding process, polyelectrolyte complexes, and others [11,14]. The materials for encapsulation should be biocompatible, of constant quality with the surrounded cells and the host. The membrane of capsules must be semipermable with adequate mechanical strength to survive implantation, the biochemical, and biological stresses from the patient. The membrane can be single or multilayer of natural and synthetic polymers [14,15]. The most commonly microcapsules are based on an alginate core surrounded by a polycation layer which at the same time is covered by an outer alginate membrane [11,14–17]. Polycations, such as, poly-L-lysine [18], poly-L-ornithine [19], chitosan [20,21], lactose modified chitosan [22,23], and photopolymerized biomaterials [24] improve the stability and biocompatility [11,25]. Unfortunately, they have a very low mechanical strength that can cause the release of the cells and immunization of the host (second set effect) that seriously hindering further therapy [26,27]. Synthetic, biocompatible polymers like polyurethane, polylactic acid, polyglycolic acid, poly(ether-sulfone), polysulfone [11,15,17,29–33] or their copolymers poly (D,L-lactic-co-glycolic acid) (PLGA) [34] can be used for microcapsulation process. They have advantages like easy synthesize in large quantities opposite to natural polymers, they can be more easily engineered for desired properties and they have better mechanical properties than natural polymers. This avoids the risk of cracking of microcapsules coating of immobilized cells during and after implantation [15]. However, the polysulfone and polyethersulfone (PES) as hydrophobic polymers are prone to fouling, especially by protein. In order to improve the hydrophilicity of surface, porosity, and pore connection of PSf UF membrane, many attempts of modifications have been made, including surface grafting (adsorption reaction, chemical reaction, and plasma surface grafting), coating, and polymer blending [35–39]. The best results were obtained using Pluronic as an additive to increase hydrophilicity of membranes [40–43]. However, so far there is no information about the development of the membrane of durable biocompatible polymers which, when implanted for a long time maintain constant permeability. The membranes with stable permeation properties are needed to encapsulate cells for implantation.

In our research, we assume that it is possible to develop a membrane which, despite biological fouling, would maintain constant permeability and a cut-off point for a long time. In this case, the membrane should increase the hydraulic permeability over time. The solution can be to remove one of the polymers from the membrane. This can be done, for example, by chemical removal of polyvinylpyrrolidone [44] or polyimide [45]. In our first work, we developed hollow fiber from a mixture of polysulfone and cellulose acetate [46]. Removal of cellulose acetate from the membrane by hydrolysis confirmed our concept. We made another hollow fiber from a polysulfone-polyurethane mixture where polyurethane was hydrolyzed. This allowed for increased hydraulic permeability without changing the cut off [47]. A mixture of PES and co-poly(glycolide-ε-caprolactone) was also used to obtain microcapsules [30].

The purpose of this work was to develop a new semipermable membrane made of a polymer mixture: polysulfone as a stable polymer and biodegradable terpolymer, L-lactide, ε-caprolactone, and glycolide [48]. The choice of these compounds was due to the biocompatibility of both polymers. To our knowledge, this type of membrane has not been studied or described by anyone except our team has not yet been described.

2. Materials and methods

2.1. Chemicals and materials

Unless otherwise specified, all reagents and chemicals were of analytical grade. PSE 6020 was purchased from BASF and dried under vacuum at 110°C by 8 h; PVP 10 kDa, BSA, dry chloroform and methanol, inulin, trypsin, PEG 35 kDa, Pluronic F 127, zirconium(IV) acetylacetonate, eggs albumin, and casein were purchased from Sigma-Aldrich (St. Louis, MO). *N*-methylpyrolidone (NMP), tetrahydrofuran (THF) were purchased from Merck. L-Lactide, glycolide (Glaco Ltd., China) were purified by recrystallization from ethyl acetate solution and dried in a vacuum oven at room temperature. ε-Caprolactone (ε-CL) (across organics) was distilled under reduced pressure from freshly powdered calcium hydride before use. The deionized water (18.2 MΩ cm) was produced using Mili-Q apparatus (Milipore).

2.2. Synthesis of L-lactide/glycolide/e-caprolactone terpolymer (LGC) at bulk

The synthesis of the terpolymer was based on our previously described method of ROP conducted with the use of $Zr(acac)_4$ as a low toxic and efficient initiator [49]. Sealed glass two-necked flask (250 mL), equipped with a magnetic stirrer and argon inlet with gas exhaust system was used as a reaction vessel. L-Lactide, glycolide, and e-caprolactone was weighed into the reaction vessel. After the melting of the content of vessel at 110°C, a measured volume of initiator solution was added to the vessel. Then, the reaction vessel was closed with a glass stopper and kept in a thermostatically controlled oil bath at 110°C–120°C until reaction completion (48 h). After a selected reaction time, the vessel was quickly quenched to room temperature. The resulting terpolymer was purified from residual monomer by dissolving in chloroform and dropwise addition of the resulting solution to cold methanol. Purified material, after drying in a vacuum oven at room temperature, was subjected to further studies.

The initial comonomers molar ratio L-La:Gly:Cap was 70:10:20. We obtained a crude product with total conversion of monomers about 98%. The composition of the final purified product was: 72% of lactid, 12% of glycolid, and 16% of ε-caprolactone units. The number average

molecular mass of the terpolymer was 110 g/mol with molar mass dispersion 2.9.

The main factor forming the final microstructure of the obtained terpolymer is the processes of intermolecular transesterification proceeding during the actual terpolymerization reaction. The relatively low temperature of terpolymerization was applied to obtain special multiblock segmental chain microstructure of the synthesized terpolymer by specific intermolecular transesterification mechanism and its low intensity [49,50]. These processes provoke the formation of segmental microstructure of the chain resembling a "diblock structure," consisting of lactidyl microblocks and microblocks of the random glycolide/caprolactone copolymer. Using the previously developed methods for determining the structure of the terpolymer chain based on the results of NMR [49], we determined the average length of lactidyl, glycolidyl, and caproyl microblocks in terpolymer chains respectively as: 6.1 lactidyl units, 0.6 glycolidyl units, and 1.0 caproyl units. The obtained terpolymer had a multiblock, segmental microstructure.

2.2.1. Terpolymer characterization

The composition and microstructure of the terpolymer chain were determined on the basis of NMR spectra obtained with Bruker Avans spectrometer (600 MHz) in dimethyl sulfoxide-d_6 (DMSO), in the presence of tetramethylsilane as internal chemical shift standard.

Average number molecular weights (M_n) and dispersion indexes (D) of the synthesized polymer samples were measured using gel permeation chromatography (GPC) (Viscotek apparatus Rimax, chloroform, temperature 35°C, flow 1 mL/min, using two Viscotek 3580 columns, refractive detector, and calibration with polystyrene standards).

2.3. Membrane casting by phase inversion method

Membranes were prepared from casting mixtures obtained by blending two solutions *A* and *B*, according to the compositions listed below. The solutions were prepared under dry nitrogen in 500 mL tightly closed flask and heated to approximately 45°C while being stirred with cross-shaped stirring bars at 60 rpm using a stirring hot plate. The polymers dissolve completely within 24 h. Then, polymers were stirred for at least further 24 h, the resulting solutions were blended and degassed under reduced pressure (1 kPa). The mixtures after degassing were immediately cast on a glass plate with a steel knife at thickness of 250 μm and after 20 min of drying on air (30%–35% relative humidity, 22°C–23°C, air conditioned laboratory) the glass plate was immersed in a coagulation bath of deionized water. The formed membranes after one hour were transferred to a second bath and subsequently washed again with deionized water for 24 h to remove solvents and pore-forming agents. Then, membranes were dried on air for 8 h and then dried under reduced pressure (0.5 kPa) for 2 h and stored in a tightly closed flask with molecular sieves 4 A before use in experiments.

Solution *A*: 18 g PES, 9 g PVP 10 kD, 3 g Pluronic 127, and 70 g NMP; solution *B*: 18 g LGC, 9 g PVP 10 kD, 3 g Pluronic 127, and 70 g THF.

The membrane casting solution composition v/v:

- *M*1 – 95% *A* and 5% *B*
- *M*2 – 90% *A* and 10% *B*
- *M*3 – 85% *A* and 15% *B*
- *M*4 – 80% *A* and 20% *B*

2.4. Membrane characterization

2.4.1. SEM analysis

Scanning electron microscopy (SEM) (Hitachi TM1000) was used for imaging the membrane surface and cross-sectional morphologies. Membrane samples were first immersed in ethanol and fractured in liquid nitrogen. The membranes were fixed on stubs with carbon self-adhesive tapes. The sample was coated with a 7–10 nm layer of gold using K550X Sputter Coater apparatus. Coated samples were examined at different magnifications at an acceleration voltage of 15 kV.

2.4.2. Atomic force microscopy measurements (Surface imaging)

All atomic force microscopy (AFM) measurements were done using the commercially available system XE120 (Park Systems, Korea) under an ambient atmosphere. Topography measurements of each membrane surface were carried out in contact mode on randomly chosen regions of the sample surface. Several images at various positions were taken for each sample to gain better knowledge of the variations of local structures. For all images we started from the same values of scan parameters (scan rate was 1 Hz and set point was set to 1.0 nN), however, in each case, final optimizations were performed. The silicon nitride cantilevers with the measured spring constant of 0.0102 N/m and tip radius of 20 nm (MLCT, Bruker) were used for surface imaging.

2.4.3. Liquid sessile drop contact angle analysis

The static water contact angle was measured at room temperature (22°C–23°C) using contact angle goniometer Krőss SDA25 (Germany). Each measurement was repeated 10 times and the presented value was the average of these measurements. The membranes were air-dried at least 24 h before the measurements.

2.4.4. IR spectrometry

IR spectra were recorded on a Varian Excalibur FTIR spectrometer over the ATR element with the diamond crystal. Dried samples were placed on the crystal and press to it with the strength of 2 kG.

2.5. Ultrafiltration and retention experiments

A flow cell of a filtration system connected with a water reservoir and air controlled pressure system was designed to characterize the filtration performance of the membranes. The system consisted of a filtration rectangular 95 mm × 35 mm cell. The feed side of the system was

pressed by the air. All the ultrafiltration experiments were carried out at 22°C–23°C. After the membrane was fixed, the stirred cell and solution reservoir were filled with deionized water. Each membrane was initially pressurized for 30 min at 15 kPa before use. The water flux (J_w) was calculated by weighing at a fixed time under a trans-membrane pressure of 10 kPa. The pure water flux of the membrane (hydraulic permeability) was calculated by the following equation:

$$J_w = \frac{V}{A\Delta p\Delta t} \tag{1}$$

where V was the volume of permeated water (m^3), A was membrane area (m^2), Δp was trans-membrane pressure (Pa), and Δt was time of permeation (s).

2.6. Cut off point determination

The rejection ratio (R) of compounds used for determination of the cut-off point of membranes was calculated by the following equation:

$$R(\%) = \left[1 - \frac{C_p}{C_f}\right] \times 100 \tag{2}$$

where C_p and C_f (mg/mL) were the protein concentrations of permeate and feed solutions, respectively, and they were measured using UV-VIS Hitachi spectrophotometer U3010.

2.7. Membrane hydrolysis

The membranes were weighed on an analytical balance with an accuracy of 0.1 mg and completely immersed in 250 mL deionized water (18.2 MΩ cm) in a tightly closed container. After two weeks the membranes were dried to constant weight in a stream of dry air and their weight was recorded. After weighing, they were immersed again in the same bath. In one container there was only one membrane. The loss of water was supplemented up to 250 mL.

2.8. Elemental analysis

Elemental analysis was carried out by means of a CHNS Elemental analysis model Vario EL III. Two analyses were performed for each sample.

3. Results and discussion

Casting mixtures for membranes preparation were obtained by mixing two solutions: *A* and *B*.

During the preparation of the mixture, to membrane *M*1 (95% of *A* and 5% of *B* – experimental part) a mixture showing little opalescence was obtained. The mixture used for obtaining membrane *M*2 (90% of *A* and 10% of *B*) was slightly opaque. However, the mixture for obtaining *M*3 (85% of *A* and 15% of *B*) was clearly opaque. When preparing membrane *M*4 of 80% of *A* and 20% of *B* composition, significant problems appeared. In the membrane-forming mixture clear isolation of a fine precipitate occurred. This precipitate was found to contain the co-polyester and a small amount of polysulfone. Membrane *M*4 appeared to be of very weak mechanical strength. It very easily underwent cracking and breaking. It was not possible to determine the ultrafiltration value for this membrane, since it cracked even under small overpressure. Therefore, further studies of it were abandoned, as pointless.

The structure of these membranes was studied by means of SEM and AFM. Figs. 1 and 2 show SEM images of membrane *M*1 cross-section. Small spherical inclusions were seen on fractures of this membrane. They are very well visible at a large magnification of the interior fragments of the membrane (Fig. 2). These inclusions appeared both inside smaller pores as well as on the walls of larger pores. Also in membranes *M*2 and *M*3 the presence of similar and larger inclusions was clearly visible (Fig. 3). All the inclusions had a spherical, almost a ball shape. It seems that with an increase in the content of component *B* in the casting mixture, the inclusion diameter increases. These inclusions were formed when precipitating one or both polymers when mixing solutions *A* and *B*. The opalescence observed during the mixing of solvents was actually the effect of isolation of polymer balls which after membrane formation created precisely such inclusions. The presence of such polymer balls was found also on the surface of the membrane (Fig. 4). They have adhered with the membrane strong enough that was not possible to wash them away with a stream of water applied under the pressure of 0.3 MPa. However, after hydrolysis these balls disappeared from the membrane's surface. This observation suggests that they were composed of a polymer undergoing hydrolysis or the hydrolyzing polymer was the main component. Exactly the same result of hydrolysis was inside the membranes (Fig. 5). No inclusion inside the membranes was

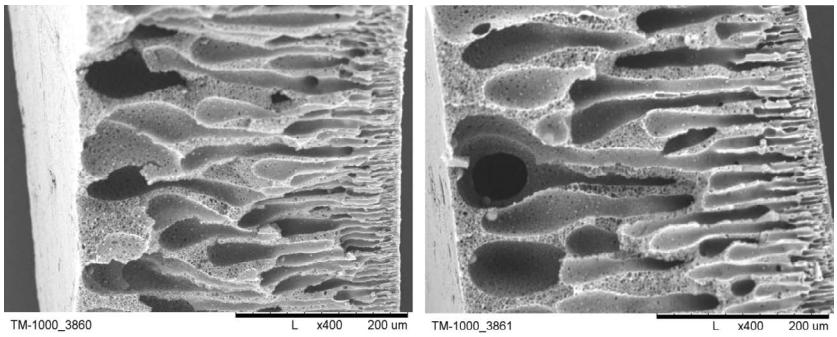

Fig. 1. Photomicrographs of membrane M1 cross-section. Magnification ×400.

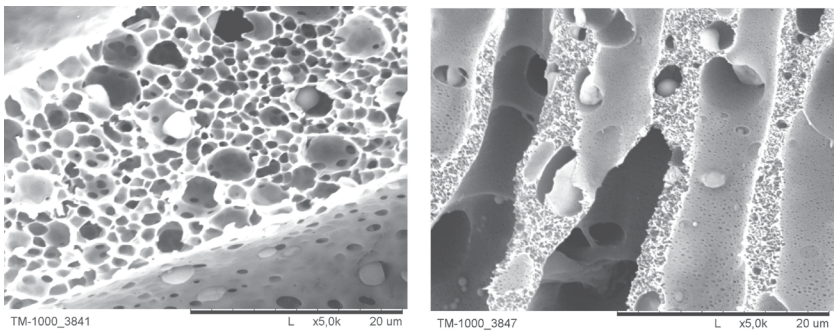

Fig. 2. Photomicrographs of cross-section of two different membranes obtained from casting mixture *M*1. Magnification ×5,000.

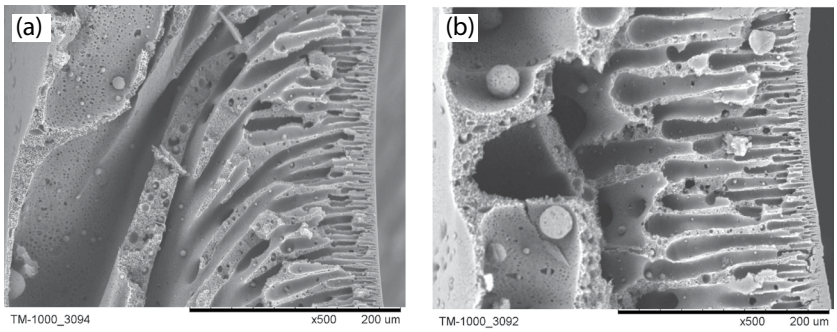

Fig. 3. Photomicrographs of membranes *M*2 (a) and *M*3 (b) cross-section. Magnification ×500.

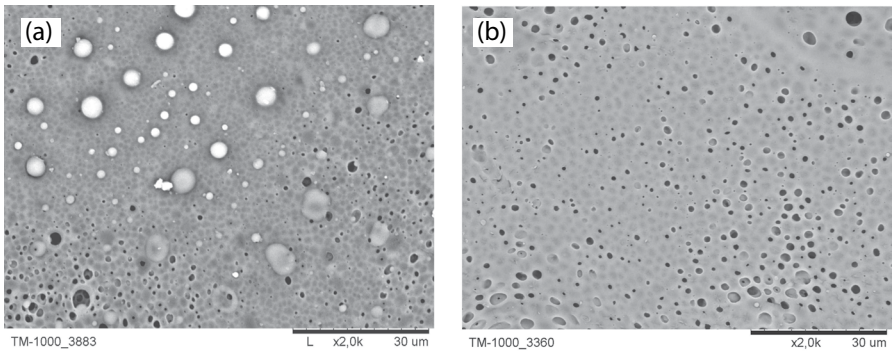

Fig. 4. Photomicrographs of membranes *M*3 surface: before hydrolysis (a) and after hydrolysis (b). Magnification ×2,000.

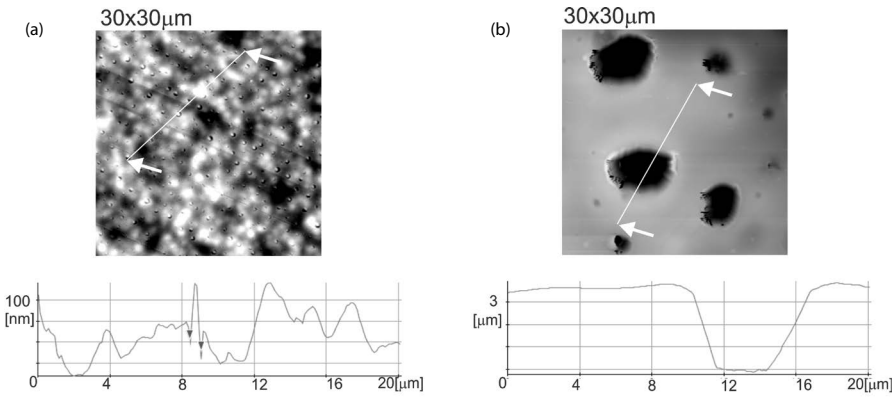

Fig. 5. AFM images and surface profiles of membranes: (a) membrane topography and the surface profile corresponding to the continuous line between grey arrows and (b) nanostructure and profile of the membrane after hydrolysis.

found after hydrolysis. The inclusions underwent hydrolysis. This clearly shows that LGC undergoing hydrolysis was their main component.

The effect of hydrolysis on the membrane surface was presented also in AFM images. They showed more details of the binding of inclusions with the membrane surface. Fig. 6 shows a typical topography obtained for membrane *M*1 before and after hydrolysis. The membrane surface profile before hydrolysis (left side) shows that the membrane surface contains many inclusions of 10–60 nm dimensions. After hydrolysis, the picture of the membrane considerably changes. The inclusions are no more visible, however, holes of 1–8 μm appear.

IR spectra were also a confirmation of the effective removal of LGC from the membrane. Fig. 7 shows two sets of fragment of the spectra. Juxtaposition *C* show the spectra of membrane *M*1. This range was selected purposefully, since the band at 1,752 cm^{-1} is the only one characteristic for LGC and does not appear for PES. This band was clear, sharp, and very intense for a membrane not subjected to hydrolysis. For membranes subjected to hydrolysis this band underwent weakening and finally completely disappeared. This confirms gradual hydrolysis of LGC and removal of the polymer remains from the membrane. The juxtaposition of spectra *D* presents the IR spectra of membranes *M*1, *M*2, and *M*3 after 20 weeks of hydrolysis and for comparison that of a membrane obtained from the casting solution *A*. The spectra of membranes *M*1, *M*2, and *M*3 were nearly identical. They differed only slightly in the intensity of the band at 1,752 cm^{-1}. This indicated an identical course of hydrolysis. The course of hydrolysis probably only slightly depended on the initial LGC content in the membrane. This is only a suggestion since this set of spectra is not a quantitative measure of the course of hydrolysis.

When comparing spectrum *D* of juxtaposition *C* recorded for membrane *M*1 after 48 weeks of hydrolysis with spectrum d of juxtaposition *D* recorded for the membrane not containing LGC, only PES, it can be stated that these spectra are nearly identical. This confirms the assumption that LGC is removed from the membrane upon hydrolysis.

The hydrolysis of LGC in the membrane is a prolonged process. When applying the gravimetric method it was found that after 48 weeks ca. 95% of LCG underwent hydrolysis (Fig. 8). Practically, the same result was

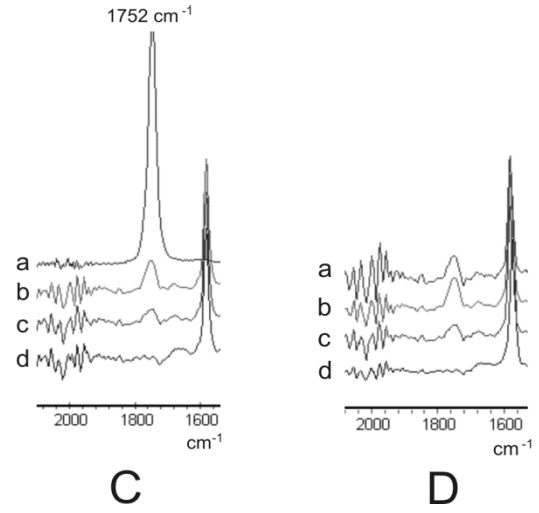

Fig. 7. IR spectra of membranes. Juxtaposition C: membrane *M*1 (a) before hydrolysis, (b) after 14 weeks of hydrolysis, (c) after 30 weeks of hydrolysis, and (d) after 46 weeks of hydrolysis. Juxtaposition D (a) membrane *M*3 after 20 weeks of hydrolysis, (b) membrane *M*2 after 20 weeks of hydrolysis, (c) membrane *M*1 after 20 weeks of hydrolysis, and (d) PES membrane obtained from 100% *A* casting solution.

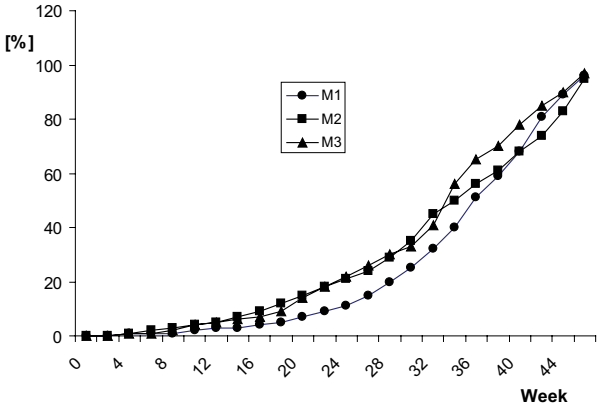

Fig. 8. Loss of weight of membranes as a function of the hydrolysis time. The loss of weight is given as a percentage loss compared to the theoretical content of the polymer LGC.

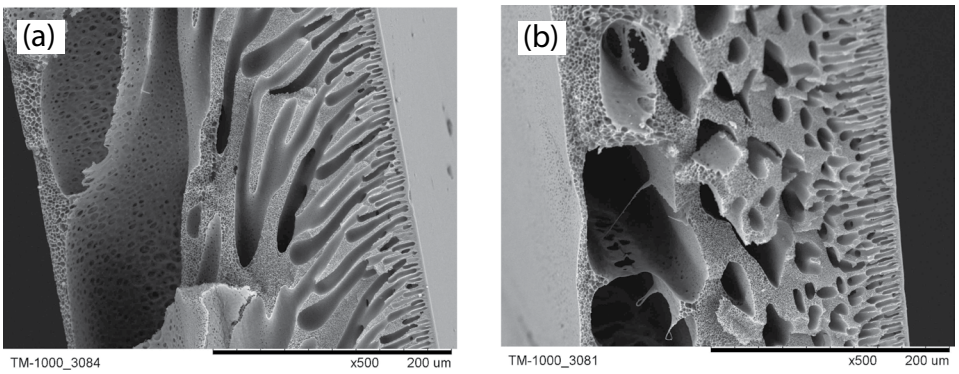

Fig. 6. Photomicrographs of cross-section of membranes after hydrolysis: *M*2 (a) and *M*3 (b) Magnification ×500.

obtained for all three membranes. The curves presenting the course of hydrolysis are very similar for all the membranes. Slight differences may result from the structure of membranes (presence of inclusions). The shape of curves may be affected by the relative humidity of air during measurements. Well dried membranes absorb moisture. This also caused a certain error in measurement, suggesting the removal of a lesser amount of LCG than actually was removed. However, these differences did not affect the general regularity. It can be assumed that the course of hydrolysis for these membranes was the same. Additional errors to the gravimetric method are introduced by the loss of PVP and Pluronic present in the membranes. Attempts were made to estimate the effect of PVP and Pluronic removal during LGC hydrolysis on the gravimetric method. The loss of Pluronic – an agent strongly hydrophilizing the membrane, should cause an increase in the contact angle. The loss of PVP from the membrane can be easily determined by elemental analysis, comparing the amount of sulfur (occurring only in PES) with the amount of nitrogen (only in PVP). PVP was used as a typical precursor of pores. Since both PES and LGC are hydrophobic, Pluronic was added to hydrophilize the membranes obtained. Pluronic enables the hydrolysis of LPG from membranes without the necessity of hydrophilization with alcohol. The contact angles for membranes before hydrolysis were: for *M*1 46.2 ± 0.40; for *M*2 48.4 ± 0.50; and for *M*3 47.9 ± 0.40. The contact angles for analogous membranes prepared without using Pluronic, but with PVP, were 66.7 ± 0.60; 74.4 ± 0.50; and 80.2 ± 0.50, respectively. For comparison, the contact angle of the membrane made with pristine LGC was 86.00 ± 0.50.

Table 1
Elemental analysis of membrane *M*2

Membrane *M*2	*N*	*S*	*S*/*N*
Before hydrolysis	0.20	2.67	13.35
After hydrolysis	0.22	3.01	14.33

Results show as mass percentage of sample.

The contact angles of membranes after hydrolysis were: for *M*1 51.2 ± 0.50; for *M*2 50.9 ± 0.40; and for *M*3 51.7 ± 0.50. An increase in wetting results in each case in loss of some amount of Pluronic from the membrane. This of course causes a certain error in the gravimetric method. This error indicated a greater loss of LGC mass that actually took place. Elemental analysis of membrane *M*2 before hydrolysis and after 48 weeks of hydrolysis was carried out in order to estimate the magnitude of PVP loss from the membrane during hydrolysis. It appeared that the ratio of sulfur to nitrogen content underwent only a slight increase, which proves that the loss of PVP is proportionally smaller than that of LGC. Therefore, it should be assumed that the loss of PVP has no considerable effect on the shape of the curve of gravimetric measurements illustrating the loss of weight of membranes.

However, the results of studies of filtration parameters are most important for evaluation of the membranes obtained. Table 2 presents the results of measurements of cut-off points before and after hydrolysis. It appeared that the values of cut-off points of membranes before and after hydrolysis hardly changed. After 46 weeks, for membrane *M*1 the cut-off point increased by 4 kDa, which is actually within the error limits. Also for membrane *M*2, the change was small and it was equal to 6 kDa. Only for membrane *M*3, the increase of 9 kDa can be assumed as considerable. However, in all three cases it did not exceed 67 kDa, that is, the value for human albumin. It appeared that removal upon hydrolysis of one of the polymers being a component of the membrane can be carried out without changing considerably the cut-off point of the membrane.

However, hydraulic permeability (ultrafiltration) measurements for the same membranes before and after hydrolysis differ between each other considerably. A considerable increase in the UF value in time was observed. For membrane *M*1 the increase after 46 weeks, that is, after nearly complete hydrolysis of LGC, was 32%. For membrane *M*2 after the same time, UF increased by 41%, and for membrane *M*3 by as much as 48%. These are very essential values. They show that such membranes may to some extent compensate for the effect of fouling after implanting them to live organisms.

Table 2
Cut off (kDa) of freshly prepared membranes and membranes after hydrolysis

Membrane	New	After 14 weeks	After 30 weeks	After 46 weeks
*M*1	42	42	44	46
*M*2	44	44	46	50
*M*3	43	44	47	52

Table 3
Hydraulic permeability (UF) (m/s Pa) of freshly prepared membranes and membranes after hydrolysis

Membrane	New	After 14 weeks	After 30 weeks	After 46 weeks
*M*1	12.29×10^{-6}	13.03×10^{-6}	14.63×10^{-6}	16.22×10^{-6}
*M*2	13.08×10^{-6}	13.99×10^{-6}	16.09×10^{-6}	18.54×10^{-6}
*M*3	12.91×10^{-6}	14.33×10^{-6}	16.39×10^{-6}	19.11×10^{-6}

4. Conclusions

A method of obtaining membranes from a mixture: polymer – stable polymer undergoing hydrolysis has been elaborated. Such membranes will very probably undergo degradation during implantation to live organisms. Since all materials used for obtaining the membranes are biocompatible, then surely these membranes could be obtained in a non-cytotoxic and biocompatible form. The LGC copolyester undergoes degradation to products which are not harmful for live organisms and will not be a threat after implantation.

The removal of the polymer from the membrane undergoing hydrolysis (biodegradation) did not cause an essential increase in the membrane cut-off point value. However, it caused an essential increase in hydraulic permeability.

Such unique properties of the membrane cause that it may at least partly compensate for the albumin fouling occurring always after implantation of the membrane to live organisms. Therefore, such types of membranes may be used for encapsulation of animal, human, and bacteria live cells and genetically modified cells. Such membranes may find application in medicine and biotechnology, where biological fouling is one of the most important problems.

Acknowledgments

The project was supported by a grant of the Institute of Biocybernetics and Biomedical Engineering No. ST/19.2.1.

References

[1] R. Lanza, R. Langer, J. Vacanti, Principles of Tissue Engineering, 2nd ed., Academic Press, San Diego, 2007.
[2] R.H. Fang, Y. Jiang, J.C. Fang, L. Zhang, Cell membrane-derived nanomaterials for biomedical applications, Biomaterials, 128 (2017) 69–83.
[3] V. Guduric, M. Fénelon, J.-C. Fricain, S. Catros, Membrane scaffolds for 3D cell culture, Curr. Trends Future Dev. Biomembr., (2020) 157–189, doi: 10.1016/B978-0-12-814225-7.00007-3.
[4] S. Novelli, C. Engelman, V. Piemonte, Membrane application for liver support devices, Curr. Trends Future Dev. Biomembr., (2020) 21–44, doi: 10.1016/B978-0-12-814225-7.00002-4.
[5] F. Ahmadi, R. Giti, S. Mohammadi-Samani, F. Mohammadi, Biodegradable scaffolds for cartilage tissue engineering, Galen Med. J., 6 (2017) 70–80.
[6] D.J. Mooney, T. Boontheekul, R. Chen, K. Leach, Actively regulating bioengineered tissue and organ formation, Orthod. Craniofacial Res., 8 (2005) 141–144.
[7] M.P. Lutolf, J.A. Hubbell, Synthetic biomaterials as instructive extracellular microenvironments for morphogenesis in tissue engineering, Nat. Biotechnol., 23 (2005) 47–55.
[8] F.M. Chen, X. Liu, Advancing biomaterials of human origin for tissue engineering, Prog. Polym. Sci., 53 (2016) 86–168.
[9] G. Turnbull, J. Clarke, F. Picard, P. Riches, L. Jia, F. Han, B. Li, W. Shu, 3D bioactive composite scaffolds for bone tissue engineering, Bioact. Mater., 3 (2018) 278–314.
[10] Y. Liu, J. Luo, X. Chen, W. Liu, T. Chen, Cell membrane coating technology: a promising strategy for biomedical applications, Nano Microlett., 11 (2019), doi: 10.1007/s40820-019-0330-9.
[11] M. Farina, J.F. Alexander, U. Thekkedath, M. Ferrari, A. Grattoni, Cell encapsulation: overcoming barriers in cell transplantation in diabetes and beyond, Adv. Drug Deliv. Rev., 139 (2019) 92–115.
[12] G. Orive, D. Emerich, A. Khademhosseini, S. Matsumoto, R.M. Hernández, J.L. Pedraz, T. Desai, R. Calafiore, P. de Vos, Engineering a clinically translatable bioartificial pancreas to treat type I diabetes, Trends Biotechnol., 36 (2018) 445–456.
[13] O.M. Sabek, M. Farina, D.W. Fraga, S. Afshar, A. Ballerini, C.S. Filgueira, U.R. Thekkedath, A. Grattoni, A.O. Gaber, Three-dimensional printed polymeric system to encapsulate human mesenchymal stem cells differentiated into islet-like insulin-producing aggregates for diabetes treatment, J. Tissue Eng., 7 (2016), doi: 10.1177/2041731416638198.
[14] M.A.J. Mazumder, Bio-encapsulation for the immune-protection of therapeutic cells, Adv. Mater. Res., 810 (2013) 1–39.
[15] P. De Vos, H.A. Lazarjani, D. Poncelet, M.M. Faas, Polymers in cell encapsulation from an enveloped cell perspective, Adv. Drug Deliv. Rev., 67–68 (2014) 15–34.
[16] J.A.M. Steele, J.P. Hallé, D. Poncelet, R.J. Neufeld, Therapeutic cell encapsulation techniques and applications in diabetes, Adv. Drug Deliv. Rev., 67–68 (2014) 74–83.
[17] F. Asghari, M. Samiei, K. Adibkia, A. Akbarzadeh, S. Davaran, Biodegradable and biocompatible polymers for tissue engineering application: a review, Artif. Cells Nanomed. Biotechnol., 45 (2017) 185–192.
[18] S.R. Bhatia, S.F. Khattak, S.C. Roberts, Polyelectrolytes for cell encapsulation, Curr. Opin. Colloid Interface Sci., 10 (2005) 45–51.
[19] C.G. Thanos, R. Calafiore, G. Basta, B.E. Bintz, W.J. Bell, J. Hudak, A. Vasconcellos, P. Schneider, S.J. Skinner, M. Geaney, P. Tan, R.B. Elliot, M. Tatnell, L. Escobar, H. Qian, E. Mathiowitz, D.F. Emerich, Formulating the alginate–polyornithine biocapsule for prolonged stability: evaluation of composition and manufacturing technique, J. Biomed. Mater. Res. Part A, 83 (2007) 216–224.
[20] L. Baruch, M. Machluf, Alginate–chitosan complex coacervation for cell encapsulation: effect on mechanical properties and on long-term viability, Biopolymers, 82 (2006) 570–579.
[21] S. Yan, M.M. Tu, Y.R. Qiu, The hemocompatibility of the modified polysulfone membrane with 4-(chloromethyl)benzoic acid and sulfonated hydroxypropyl chitosan, Colloids Surf., B, 188 (2019), doi: 10.1016/j.colsurfb.2019.110769.
[22] E. Marsich, M. Borgogna, I. Donati, P. Mozetic, B.L. Strand, S.G. Salvador, F. Vittur, S. Paoletti, Alginate/lactose-modified chitosan hydrogels: a bioactive biomaterial for chondrocyte encapsulation, J. Biomed. Mater. Res. Part A, 84 (2008) 364–376.
[23] I. Donati, I.J. Haug, T. Scarpa, M. Borgogna, K.I. Draget, G. Skjåk-Bræk, S. Paoletti, Synergistic effects in semidilute mixed solutions of alginate and lactose-modified chitosan (chitlac), Biomacromolecules, 8 (2007) 957–962.
[24] B. Baroli, Photopolymerization of biomaterials: issues and potentialities in drug delivery, tissue engineering, and cell encapsulation applications, J. Chem. Technol. Biotechnol., 81 (2006) 491–499.
[25] S. Ponce, G. Orive, R. Hernández, A.R. Gascón, J.L. Pedraz, B.J. de Haan, M.M. Faas, H.J. Mathieu, P. de Vos, Chemistry and the biological response against immunoisolating alginate-polycation capsules of different composition, Biomaterials, 27 (2006) 4831–4839.
[26] T. Orłowski, E. Godlewska, M. Tarchalska, J. Kinasiewicz, M. Antosiak, M. Sabat, The influence of immune system stimulation on encapsulated islet graft survival, Arch. Immunol. Ther. Exp., 53 (2005) 180–184.
[27] T. Orłowski, E. Godlewska, M. Mościcka, E. Sitarek, The influence of intraperitoneal transplantation of free and encapsulated langerhans islets on the second set phenomenon, Artif. Organs, 27 (2003) 1062–1067.
[28] D. Lewińska, A. Chwojnowski, C. Wojciechowski, B. Kupikowska-Stobba, M. Grzeczkowicz, A. Weryński, Electrostatic droplet generator with 3-coaxial-nozzle head for micro-encapsulation of living cells in hydrogel covered by synthetic polymer membranes, Sep. Sci. Technol., 47 (2012) 463–469.
[29] B. Kupikowska, D. Lewińska, K. Dudziński, J. Jankowska-Śliwińska, M. Grzeczkowicz, C. Wojciechowski, A. Chwojnowski, Influence of changes in composition of the membrane-forming solution on the structure of alginate-polyethersulfone microcapsules, Biocybern. Biomed. Eng., 29 (2009) 61–69.

[30] M. Grzeczkowicz, D. Lewińska, A method for investigating transport properties of partly biodegradable spherical membranes using vitamin B12 as the marker, Desal. Water Treat., 128 (2018) 170–178.
[31] G. Khang, H.B. Lee, J.B. Park, Biocompatibility of polysulfone I. surface modifications andcharacterizations, Biomed. Mater. Eng., 5 (1995) 245–258.
[32] J.Y. Ho, T. Matsuura, J.P. Santerre, The effect of fluorinated surface modifying macromolecules on the surface morphology of polyethersulfone membranes, J. Biomater. Sci. Polym. Ed., 11 (2000) 1085–1104.
[33] M. Hayama, K.I. Yamamoto, F. Kohori, K. Sakai, How polysulfone dialysis membranes containing polyvinylpyrrolidone achieve excellent biocompatibility?, J. Membr. Sci., 234 (2004) 41–49.
[34] Y.X.J. Ong, L.Y. Lee, P. Davoodi, C.H. Wang, Production of drug-releasing biodegradable microporous scaffold using a two-step micro-encapsulation/supercritical foaming process, J. Supercrit. Fluids, 133 (2018) 263–269.
[35] A. Higuchi, K. Shirano, M. Harashima, B.O. Yoon, M. Hara, M. Hattori, K. Imamura, Chemically modified polysulfone hollow fibers with vinylpyrrolidone having improved blood compatibility, Biomaterials, 23 (2002) 2659–2666.
[36] K.S. Kim, K.H. Lee, K. Cho, C.E. Park, Surface modification of polysulfone ultrafiltration membrane by oxygen plasma treatment, J. Membr. Sci., 199 (2002) 135–145.
[37] S. Zhao, Z. Wang, J. Wang, S. Yang, S. Wang, PSf/PANI nanocomposite membrane prepared by *in situ* blending of PSf and PANI/NMP, J. Membr. Sci., 376 (2011) 83–95.
[38] W. Zhao, J. Huang, B. Fang, S. Nie, N. Yi, B. Su, H. Li, C. Zhao, Modification of polyethersulfone membrane by blending semi-interpenetrating network polymeric nanoparticles, J. Membr. Sci., 369 (2011) 258–266.
[39] W. Zhao, Y. Su, C. Li, Q. Shi, X. Ning, Z. Jiang, Fabrication of antifouling polyethersulfone ultrafiltration membranes using Pluronic F127 as both surface modifier and pore-forming agent, J. Membr. Sci., 318 (2008) 405–412.
[40] A.M. Isloor, B.M. Ganesh, S.M. Isloor, A.F. Ismail, H.S. Nagaraj, M. Pattabi, Studies on copper coated polysulfone/modified poly isobutylene alt-maleic anhydride blend membrane and its antibiofouling property, Desalination, 308 (2013) 82–88.
[41] Y.Q. Wang, T. Wang, Y.L. Su, F.B. Peng, H. Wu, Z.Y. Jiang, Remarkable reduction of irreversible fouling and improvement of the permeation properties of poly(ether sulfone) ultrafiltration membranes by blending with pluronic F127, Langmuir, 21 (2005) 11856–11862.
[42] K.A. Faneer, R. Rohani, A.W. Mohammad, Influence of pluronic addition on polyethersulfone membrane for xylitol recovery from biomass fermentation solution, J. Cleaner Prod., 171 (2018) 995–1005.
[43] Y. Zhang, X. Tong, B. Zhang, C. Zhang, H. Zhang, Y. Chen, Enhanced permeation and antifouling performance of polyvinyl chloride (PVC) blend Pluronic F127 ultrafiltration membrane by using salt coagulation bath (SCB), J. Membr. Sci., 548 (2018) 32–41.
[44] J.J. Qin, F.S. Wong, Hypochlorite treatment of hydrophilic hollow fiber ultrafiltration membranes for high fluxes, Desalination, 146 (2002) 307–309.
[45] Y. Ding, B. Bikson, Macro and meso porous polymeric materials from miscible polysulfone/polyimide blends by chemical decomposition of polyimides, Polymer, 51 (2010) 46–52.
[46] C. Wojciechowski, A. Chwojnowski, L. Granicka, E. Łukowska, Polysulfone/cellulose acetate blend semi degradable capillary membranes preparation and characterization, Desal. Water Treat., 64 (2017) 365–371.
[47] W. Sikorska, C. Wojciechowski, M. Przytulska, G. Rokicki, M. Wasyłeczko, J.L. Kulikowski, A. Chwojnowski, Polysulfone–polyurethane (PSf-PUR) blend partly degradable hollow fiber membranes: preparation, characterization, and computer image analysis, Desal. Water Treat., 128 (2018) 383–391.
[48] E. Pamuła, P. Dobrzyński, M. Bero, C. Paluszkiewicz, Hydrolytic degradation of porous scaffolds for tissue engineering from terpolymer of L-lactide, ε-caprolactone and glycolide, J. Mol. Struct., 744–747 (2005) 557–562.
[49] P. Dobrzynski, Synthesis of biodegradable copolymers with low-toxicity zirconium compounds. III. Synthesis and chain-microstructure analysis of terpolymer obtained from L-lactide, glycolide, and ε-caprolactone initiated by zirconium(IV) acetylacetonate, J. Polym. Sci., Part A: Polym. Chem., 40 (2002) 3129–3143.
[50] P. Dobrzynski, Synthesis of biodegradable copolymers with low-toxicity zirconium compounds. II. Copolymerization of glycolide with ε-caprolactone initiated by zirconium(IV) acetylacetonate and zirconium(IV) chloride, J. Polym. Sci., Part A: Polym. Chem., 40 (2002) 1379–1394.